Biochemistry

Article

Cite This: *Biochemistry* 2019, 58, 1155−1166

pubs.acs.org/biochemistry

Glycosaminoglycan Compositional Analysis of Relevant Tissues in Zika Virus Pathogenesis and *in Vitro* Evaluation of Heparin as an Antiviral against Zika Virus Infection

So Young Kim,[†] Cheri A. Koetzner,[‡] Anne F. Payne,[‡] Gregory J. Nierode,[§] Yanlei Yu,[†] Rufeng Wang,[§] Evan Barr,[⊥] Jonathan S. Dordick,[†,§,⊥,#] Laura D. Kramer,[‡,@] Fuming Zhang,*[,§] and Robert J. Linhardt*[,†,§,⊥,#,∥]

[†]Biochemistry and Biophysics Graduate Program, Center for Biotechnology and Interdisciplinary Studies, Rensselaer Polytechnic Institute, Troy, New York 12180, United States

[‡]Wadsworth Center, New York State Department of Health, Slingerlands, New York 12159, United States

[§]Department of Chemical and Biological Engineering, Center for Biotechnology and Interdisciplinary Studies, Rensselaer Polytechnic Institute, Troy, New York 12180, United States

[∥]Department of Chemistry and Chemical Biology, Center for Biotechnology and Interdisciplinary Studies, Rensselaer Polytechnic Institute, Troy, New York 12180, United States

[⊥]Department of Biological Science, Center for Biotechnology and Interdisciplinary Studies, Rensselaer Polytechnic Institute, Troy, New York 12180, United States

[#]Department of Biomedical Engineering, Center for Biotechnology and Interdisciplinary Studies, Rensselaer Polytechnic Institute, Troy, New York 12180, United States

[@]State University of New York at Albany School of Public Health, Albany, New York 12222, United States

Supporting Information

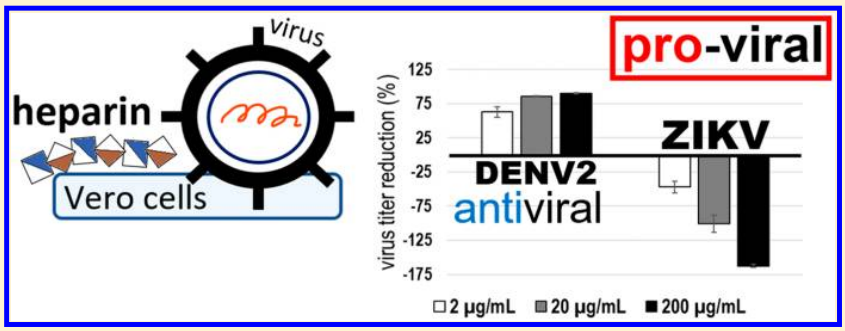

ABSTRACT: Zika virus (ZIKV) is an enveloped RNA virus from the flavivirus family that can cause fetal neural abnormalities in pregnant women. Previously, we established that ZIKV-EP (envelope protein) binds to human placental chondroitin sulfate (CS), suggesting that CS may be a potential host cell surface receptor in ZIKV pathogenesis. In this study, we further characterized the GAG disaccharide composition of other biological tissues (i.e., mosquitoes, fetal brain cells, and eye tissues) in ZIKV pathogenesis to investigate the role of tissue specific GAGs. Heparan sulfate (HS) was the major GAG, and levels of HS-6-sulfo, HS 0S (unsulfated HS), and CS 4S disaccharides were the main differences in the GAG composition of *Aedes aegypti* and *Aedes albopictus* mosquitoes. In human fetal neural progenitor and differentiated cells, HS 0S and CS 4S were the main disaccharides. A change in disaccharide composition levels was observed between undifferentiated and differentiated cells. In different regions of the bovine eyes, CS was the major GAG, and the amounts of hyaluronic acid or keratan sulfate varied depending on the region of the eye. Next, we examined heparin (HP) of various structures to investigate their potential *in vitro* antiviral activity against ZIKV and Dengue virus (DENV) infection in Vero cells. All compounds effectively inhibited DENV replication; however, they surprisingly promoted ZIKV replication. HP of longer chain lengths more strongly promoted activity in ZIKV replication. This study further expands our understanding of role of GAGs in ZIKV pathogenesis and carbohydrate-based antivirals against flaviviral infection.

Once believed to be a benign virus, Zika virus (ZIKV) has cumulatively led to >200000 infections resulting in a global health risk, especially in pregnant women. ZIKV is an

Received: December 11, 2018
Revised: January 29, 2019
Published: January 30, 2019

DOI: 10.1021/acs.biochem.8b01267
Biochemistry 2019, 58, 1155−1166

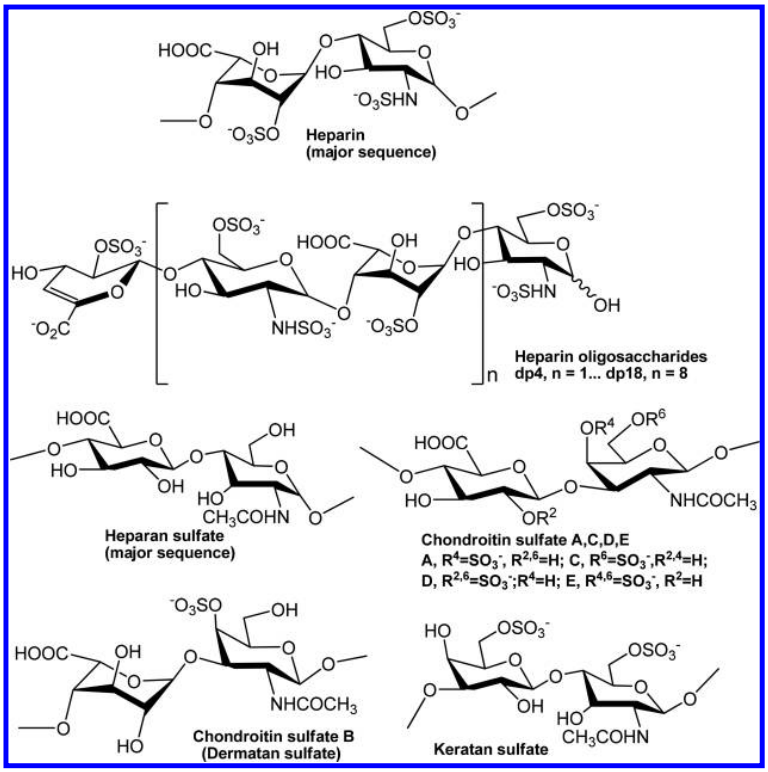

Figure 1. Structure of main GAG disaccharides.

enveloped single-stranded RNA virus of the flavivirus family like Dengue virus (DENV) and West Nile virus (WNV). The mature ZIKV particle is 50 nm in diameter, and its surface consists of 180 copies of the envelope and membrane proteins.[1] Upon adsorption by the host cell, an internalization conformation change of the envelope protein triggers membrane fusion and releases the viral genome (10.8 kb).[2] The viral RNA is translated into a single polyprotein encoding premembrane and envelope and seven nonstructural proteins (NS1, NS2A, NS2B, NS3, NS4A, NS4B, and NS5).[2] Generation of capsid and membrane protein from premembrane protein indicates the maturity of the viral particle, which then exits the host cell. ZIKV has various transmission routes, including bodily fluids, sexual transmission, and mosquito vectors.[3−5] In addition, ZIKV has a detrimental ability to cross the placental barrier and cause fetal abnormalities such as microcephaly and vision loss, resulting in the appearance of ZIKV on the global health threat list of the World Health Organization in 2017. While the number of incidents significantly declined in 2018, the Centers for Disease Control and Prevention reports that one in seven children born with congenital ZIKV infection in the United States and U.S. territories developed a neurodevelopmental abnormality,[6] suggesting an ongoing need for a better understanding of ZIKV pathogenesis and the design of effective preventative therapeutics and treatment options.

Other pathogenic flaviviruses first bind to glycosaminoglycans (GAGs) through their surface envelope proteins (EPs) as a first step in their host cell invasion.[7,8] GAGs are anionic linear polysaccharides comprised of a repeating disaccharide unit with an average molecular weight ranging from 14 to 1000 kDa (Figure 1).[8] GAGs are located in an extracellular matrix linked to core proteins of proteoglycans (PGs) and in a soluble form, and they play key biological functions, including roles in cellular communication, development, immunity, and pathogenesis.[9] In our previous work, we characterized the human placental GAG composition and showed nanomolar binding interactions (K_D = 658 nM) between human placental GAGs and ZIKV-EP, suggesting that ZIKV may also utilize host cell surface GAGs as a landing patch during host cell invasion like DENV.[10] We also identified high-affinity heparan sulfate (HS) and chondroitin sulfate (CS) disaccharides against ZIKV-EP. However, the tissue or organism specific GAG composition from other biological tissues infected by ZIKV had not been characterized. For example, *Aedes aegypti* (AE) and *Aedes albopictus* (AL) mosquitoes are the main mosquito vectors that aid in the transmission of pathogenic flaviviruses, including DENV and ZIKV.[5] While GAGs may not be essential receptors for host cell invasion of DENV in mosquito cells, the structural GAG analysis of these *Aedes* mosquitoes had not been performed for comparison to the GAGs in mammalian cell targets.[11] Furthermore, fetal neurological abnormalities are the signature of vertical ZIKV transmission, and various neural cells are susceptible to ZIKV infection. ZIKV infects human fetal cortical neural progenitor cells, neurons, astrocytes, microglia, and oligodendrocytes, and neural progenitor cells are the preferred target of ZIKV.[12−14] Immature neurons differentiated from human neural progenitor cells show poor permissiveness to ZIKV infection.[10] Unfortunately, only GAGs in adult CNS have been studied.[15] Ocular abnormalities, including retinal, choroidal, and optic nerve abnormalities, have also been reported in infants affected by congenital ZIKV infection;[16−18] however, ocular tissue specific GAGs have not been previously analyzed. HS has been previously implicated in

DOI: 10.1021/acs.biochem.8b01267
Biochemistry 2019, 58, 1155−1166

viral and bacterial keratitis and age-related macular degeneration.[19] GAGs are generally well-conserved across mammalian species, and bovine eyes have been previously used to model the human eye.[20] In the study presented here, we perform GAG disaccharide compositional analysis of *Aedes* mosquitoes, human fetal neural progenitor and differentiated cells, and bovine eyes. These analyses rely on liquid chromatography−mass spectrometry (LC−MS) for investigation of tissue or organism specific GAGs and their potential contribution to ZIKV-EP binding.

Heparin (HP) and other sulfated GAGs inhibit the replication of various pathogenic flaviviruses, including yellow fever virus (YFV), Japanese encephalitis virus (JEV), and DENV with the EC_{50} (effective concentration) or IC_{50} (inhibitory concentration) ranging from 0.2 to 1.89 μg/mL in Vero cells.[21] HP has also been found to successfully inhibit ZIKV replication in Vero and human neural progenitor cells.[22,23] Our previous work showed that a minimal HP chain length requirement for ZIKV-EP binding was octasaccharide (dp8), and HP dodecasaccharide (dp12) competitively inhibits binding of ZIKV-EP to HP by >40% in a surface plasmon resonance competition (SPR) assay.[10] Shorter chain length HP oligosaccharides have the advantage of lower anticoagulant activities and the utility of being used as a ligand for multivalent conjugates for amplified binding;[24,25] however, the antiviral activity of HP derivatives of varying structure against flaviviral infection has not been previously investigated. The structures of commercial unfractionated heparin (HP), low-molecular weight heparin (LMWH), heparin dodecasaccharide (HP dp12), and non-anticoagulant heparin (s-NACH) vary in terms of chain length, sulfation level, and disaccharide sequence. While HP, LMWH, and HP dp12 share same major disaccharide sequence but have different chain lengths, s-NACH lacks an antithrombin binding site.[26] The average molecular weights of HP, LMWH, dp12 HP, and s-NACH are approximately 12−15, 5, 3.5, and 5 kDa, respectively. In this study, we tested these compounds to investigate the efficiency of the antiviral activity of heparin against ZIKV and DENV replication in Vero cells based on its structure.

GAG disaccharide compositional analysis of *Aedes* mosquitoes, human fetal neural progenitor cells and differentiated astrocytes, neurons, and oligodendrocytes, and bovine eye tissues based on LC−MS and their potential roles in ZIKV pathogenesis are discussed. The antiviral activities of heparin compounds with varying structures were also tested *in vitro* against ZIKV and DENV infection to determine their minimal structural requirement for efficient inhibition.

EXPERIMENTAL PROCEDURES

Materials. Unsaturated disaccharide standards of CS (ΔUA-GalNAc, ΔUA-GalNAc4S, ΔUA-GalNAc6S, ΔUA2S-GalNAc, ΔUA2S-Gal-NAc4S, ΔUA2S-GalNAc6S, ΔUA-Gal-NAc4S6S, and ΔUA2S-GalNAc4S6S), unsaturated disaccharide standards of HS (ΔUA-GlcNAc, ΔUA-GlcNS, ΔUA-GlcNAc6S, ΔUA2S-GlcNAc, ΔUA2S-GlcNS, ΔUA-GlcNS6S, ΔUA2S-GlcNAc6S, and ΔUA2S-GlcNS6S), and the unsaturated disaccharide standard of HA (ΔUA-GlcNAc), where ΔUA is 4-deoxy-α-L-*threo*-hex-4-enopyranosyluronic acid, S is sulfo, and Ac is acetyl, were from Iduron. Actinase E was obtained from Kaken Biochemicals (Tokyo, Japan). Chondroitin lyase ABC from *Proteus vulgaris* was expressed in *Escherichia coli* in our laboratory. Recombinant Flavobacterial heparinase I, II, and III were expressed in our laboratory using *E. coli* strains that were gifts from J. Liu (The University of North Carolina at Chapel Hill, Chapel Hill, NC).[27] Recombinant keratanase II from *Bacillus circulans* was expressed and purified in our laboratory, as well.[28] 2-Aminoacridone (AMAC) and sodium cyanoborohydride ($NaCNBH_3$) were obtained from Sigma-Aldrich (St. Louis, MO). All other chemicals were of high-performance liquid chromatography grade. Vivapure Q Maxi and Mini H strong anion exchange spin columns were from Sartoriou Stedim Biotech (Bohemia, NY). Amicon Ultra 0.5 and 15 mL 3K molecular weight cutoff (MWCO) centrifugal filters were purchased from MilliporeSigma (Burlington, MA). BugBuster 10× protein extraction reagent was also purchased from MilliporeSigma. Frozen bovine eyes were purchased from Bioreclamation IVT (Westbury, NY). Recombinant ZIKV-EP and DENV-EP expressed in *E. coli* were purchased from eEnzyme LLC and ProSpec-Tany TechnoGene Ltd., respectively. Human recombinant FGF1 and FGF2 expressed in *E. coli* were a gift from Amgen.

A. aegypti mosquitoes were from a laboratory colony maintained at Wadsworth Center for >5 years. *A. albopictus* mosquitoes (kindly provided by I. Rochlin, Suffolk County Health Department, Yaphank, NY) were originally collected in Suffolk County, NY, in 2014 and subsequently colonized in the New York State Department of Health Arbovirus Laboratory. They were reared and maintained at 27 °C under standard conditions before experimentation.[29]

Human Neural Progenitor Cell Culture. The *v-myc* immortalized human fetal neural progenitor cell (hNPC) line ReNcell VM and the c-myc immortalized cortical progenitor cell line (ReNcell CX) (EMD Millipore) were used for this study between passages 4 and 10. Undifferentiated hNPCs were maintained following the manufacturer's guidelines. Briefly, cells were cultured on laminin (Sigma)-coated T25 or T75 flasks in ReNcell Maintenance Medium (EMD Millipore) containing 20 ng/mL fibroblast growth factor (FGF2) (EMD Millipore), 20 ng/mL epidermal growth factor (EGF) (EMD Millipore), and 100 units/mL penicillin-streptomycin (Gibco). Cells were passaged using Accutase and replated at a density of 10000 cells/cm^2 when approximately 90% confluent. Medium was changed the day after passaging and every second day thereafter. For differentiation, undifferentiated cells were plated and expanded to 90% confluency. Upon reaching 90% confluency, cultures were changed to differentiation medium consisting of only ReNcell Maintenance Medium containing 100 units/mL penicillin-streptomycin. Medium was changed every second day during differentiation until cell isolation for GAG analysis. For cell isolation, cultures were removed from culture flasks using a sterile scraper and centrifuged at 300*g* for 7 min before the medium was decanted and the cell pellet was frozen. All cultures were maintained within incubators kept at 37 °C and 5% CO_2.

Western Blotting. Following culturing of undifferentiated and differentiated hNPCs, cells were collected using a scraper and lysed using RIPA buffer (Cell Signaling Technologies). The protein concentrations of cell lysates were estimated using a BCA assay (Sigma). Equal amounts of protein (~10 μg) were loaded into either 8 or 12% cast sodium dodecyl sulfate−polyacrylamide gel electrophoresis (SDS−PAGE) gels. These SDS−PAGE gels were resolved at 120 V in a tris-glycine buffer and electro-transferred to a nitrocellulose membrane for either 60 min at 100 V (12% gel) or overnight at 30 V (8% gel) at 4

DOI: 10.1021/acs.biochem.8b01267
Biochemistry 2019, 58, 1155−1166

°C. Membranes were rinsed with tris-buffered saline (TBS), blocked using 5% (w/v) bovine serum albumin (BSA) in TBS for 1 h at room temperature, and incubated overnight at 4 °C in antibody solutions diluted in blocking buffer with 0.05% (v/v) Tween 20. The antibodies against nestin (NES) and SOX2, glial fibrillary acidic protein (GFAP), βIII-tubulin (TUBB3), and CNPase (CNP) were used to confirm the presence of NPC, astrocytes, neurons, and oligodendrocytes, respectively. Following primary antibody incubation, membranes were rinsed with TBS containing 0.05% Tween 20 (TBST) and incubated with an appropriate secondary antibody diluted in TBS with 3% (w/v) BSA for 90 min at room temperature. These membranes were rinsed with TBST and again with TBS before being incubated with a chemiluminescence solution (SuperSignal Pico, Pierce) for 10 min. A Bio-Rad ChemiDoc was used to image the membranes for 15 s exposures (except for TUBB3, which was exposed for 60 s). After imaging, membranes were subsequently stripped using a stripping buffer [200 mM glycine, 1% (v/v) Tween 20, and 0.1% (w/v) SDS (pH 2)], evaluated for efficient stripping with a chemiluminescence solution, and rinsed with TBS before being reused with the procedure described above for detection of the loading control protein (β-actin). Densitometry image analysis was used to assess the signal intensity associated with the protein bands of the Western blot images using ImageJ.

Extraction of Glycosaminoglycans from Bovine Eyes, *Aedes* Mosquitoes, and Human Neural Progenitor Cells. Three sets of bovine eyes were thawed at 4 °C, rinsed with chilled phosphate-buffered saline (PBS), and dissected into four regions (cornea, conjunctiva, lens, and optic nerve). Each region was lyophilized and cut into smaller pieces prior to being defatted with acetone and being shaken at room temperature for 1 h. Once the acetone was completely evaporated, the tissue was digested using actinase E for 12–24 h. Completely digested tissues were lyophilized, and dry tissues were dissolved in 8 M urea and 2 wt % CHAPS {3-[(3-cholamidopropyl)dimethylammonio]-1-propanesulfonate} buffer, and GAGs were purified using MAXI H spin columns.[10] Permeate was collected and desalted using 3 kDa MWCO spin columns, and the retentate was collected and lyophilized (lyophilized GAG samples).

GAGs were extracted from *Aedes* mosquitoes using the established method in our laboratory.[30] Mosquito samples were first lyophilized, which was defatted with acetone (1 mL) while being shaken at room temperature for 1 h. Acetone was allowed to evaporate, and the pellet was extracted with a solution comprised of sodium dodecyl sulfate (SDS) (1.0 mL, 0.5%), NaOH (0.1 M), and $NaBH_4$ (0.8%) while being constantly stirred for 16 h at room temperature. Sodium acetate (200 μL of a 1 M solution) and HCl (300 μL of a 1 M solution) were then added followed by filtration. Hydrochloric acid (200 μL, 1 M) was added to the filtrate, and insoluble material was removed by centrifugation at 2500*g*. The crude GAG was collected by adding ethanol (7 mL) to the supernatant, chilled for 2 h at 0 °C, and collected by centrifugation at 2500*g* for 10 min at 4 °C. The precipitate (GAG) was dissolved in 250 μL of water and lyophilized.

Human neural progenitor cells were lysed using 100 μL of sonication buffer (BugBuster 10× protein extraction reagent) per 1 million cells and transferred into the 1 mL microcentrifuge tubes, which were placed in the sonicator at room temperature for 30 min. The cell mixture was desalted using 3K MWCO centrifuge columns and collected for GAG lyase treatment.

Digestion of GAGs into CS, HS, HA, and KS Disaccharides. Lyophilized GAG samples were treated with a mixture of recombinant heparinase I, II, and III, chondroitinase ABC, and keratanase in digestion buffer (20 milliunits of each enzyme/mg of GAG in 50 mM ammonium acetate containing 2 mM calcium chloride adjusted to pH 7.0) at 37 °C for 5 h to prepare CS, HS, and KS disaccharides. The reaction was terminated by placing the mixture in a 100 °C water bath for 5 min. The reaction mixture was cooled and centrifuged in 3 kDa spin columns to collect disaccharide products.

AMAC Labeling. The dried samples were labeled with AMAC (2-aminoacridone) by adding 10 μL of 0.1 M AMAC in a dimethyl sulfoxide/acetic acid mixture [17/3 (v/v)], incubating the samples at room temperature for 10 min, followed by addition of 10 μL of 1 M aqueous $NaBH_3CN$, and incubating the samples for 1 h at 45 °C. A mixture containing all 19 disaccharide standards prepared at 6.25 ng/μL was similarly labeled with AMAC and used for each run as an external standard. After the AMAC labeling reaction, the samples were centrifuged and each supernatant was recovered.

Disaccharide Analysis Using Liquid Chromatography–Mass Spectrometry. LC–MS analyses were performed on an Agilent 1200 LC/MSD instrument (Agilent Technologies, Inc., Wilmington, DE) equipped with a 6300 ion trap and a binary pump. The column was an Agilent Poroshell 120 C18 column (2.7 μm, 3.0 mm × 150 mm). The column temperature was 45 °C. The flow rate was 150 μL/min. The mobile phase was 50 mM NH_4OAc in water (A) and methanol (B): 5 to 30% B from 0 to 20 min, 30 to 50% B from 20 to 30 min, 100% B from 30 to 40 min, and 5% B from 40 to 50 min. The MS parameters were electrospray in negative ionization mode with a skimmer potential of −40.0 V, a capillary exit of −40.0 V, and a source temperature of 350 °C. The mass range of the spectrum was m/z 300–900. Nitrogen (8 L/min, 40 psi) was used as the drying and nebulizing gas.

Cell Culture and Virus for Plaque and Antiviral Assays. African green monkey kidney epithelial cells (Vero) were grown and maintained in EMEM with 2% FBS containing 100 μg/mL penicillin and 10 μg/mL streptomycin sulfate. ZIKV PRVABC59 (Puerto Rico 2015) and DENV2 New Guinea C strains, obtained from the Centers for Disease Control and Prevention, were used in the experiments. Stock ZIKV and DENV2 were grown in Vero cells at 37 °C and harvested at 3 or 4 days post-infection (dpi).

Plaque Assay. Vero cells (6×10^5) were seeded in six-well plates and incubated at 37 °C in 5% CO_2 for 3–4 days to produce a confluent monolayer. The cell culture medium was removed, and 10-fold serial dilutions of virus were inoculated into each well and incubated for 1 h at 37 °C. After adsorption, cell monolayers were overlaid with a 1:1 2× MEM/10% FBS mixture and 1.2% oxoid agar, allowed to solidify, and placed at 37 °C for 3 days (Zika) or 5 days (Den). An additional overlay of a 1:1 2× MEM/2% FBS mixture and 1.2% oxoid agar containing 2% neutral red agar was added and incubated overnight at 37 °C to visualize viral plaques. Plaques were counted, and the viral titer was calculated and expressed as plaque-forming units (PFU) per milliliter.

Viral Reduction Antiviral Assay. Vero cells at a density of 2×10^5 cells/well were seeded into 24-well plates and incubated at 37 °C in 5% CO_2 to produce a confluent

DOI: 10.1021/acs.biochem.8b01267
Biochemistry 2019, 58, 1155–1166

monolayer. After the cell culture medium was removed, the viral inoculum at a multiplicity of infection (MOI) of 0.1 PFU/cell and antiviral compounds prepared in 2% FBS/EMEM were added to the monolayer and incubated while being gently rocked every 15 min at 37 °C for 1 h. Heparin, low-molecular weight heparin, s-NACH, and dp12 heparin oligosaccharides were used as antiviral agents. Medium only and virus with medium served as controls. Plates were incubated at 37 °C for an additional 47 h before the virus was harvested from the supernatant. Viral titers were determined by a plaque assay. In the second set of experiments, cells were pretreated with antiviral agents 1 h prior to addition of viral inoculum and the samples were harvested 48 and 73 h post-infection.

Statistical analysis was performed with Microsoft Excel and SPSS software (IBM). All results were considered statistically significant (one asterisk) at the $p < 0.05$ level and extremely significant (two asterisks) at the $p < 0.01$ level.

RESULTS

A. aegypti (AE) and *A. albopictus* (AL) mosquitoes are well-established vectors of ZIKV, DENV, and Chikungunya virus (CHIKV) infection and transmission.[5] The major GAG was HS at 76.2 and 75.5% for AE and AL, respectively (Figure 2A). Total CS and HA were both below 20% of the GAG content for both species. AE exhibited 19.9% HS 6S, 19.7% HS NS, 36.6% HS 0S, 0.2% CS TriS, 6.7% CS 4S, and 16.9% HA (Figure 2B). Similarly, AL exhibited 15.9% HS NS, 59.6% HS 0S, 12.6% CS 4S, and 11.9% HA. HS 6S and CS triS were not detected in AL mosquitoes. Other notable differences were that AE had significantly higher levels of HS 6S while AL had significantly higher levels of HS 0S.

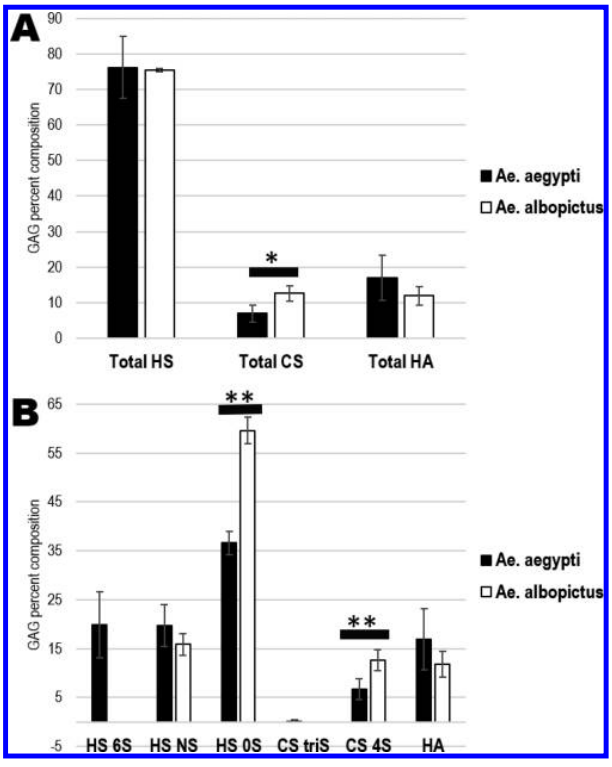

Figure 2. (A) Total GAG composition of uninfected *Aedes* mosquitoes. (B) Disaccharide composition of *Aedes* mosquitoes. GAGs from five samples containing 10 mosquitoes each were measured per mosquito species. Each sample was measured in triplicate. One asterisk and two asterisks denote the statistical comparison between *A. aegypti* and *A. albopictus* (**$p < 0.01$; * $p < 0.05$).

Human cortical neural progenitor cells had been previously reported to be susceptible to ZIKV infection.[12] Thus, we next analyzed GAGs from the ReNcell CX human neural progenitor cell line, which was derived from the cortical region of human fetal brain and immortalized. These cells readily differentiate into neurons, astrocytes, and oligodendrocytes, and we harvested GAGs from undifferentiated progenitor cells as well as 2- and 4-week differentiated cells to investigate the change in GAG composition in neural cells after the embryonic stage. In the CX cells, HS was the major GAG component, although CS and HA were also present (Figure 3A). Interestingly, the percent of HS GAG decreased from 90.4% in the undifferentiated cells to 64.4% at 4-week differentiated cells. The level of total CS, however, increased from 4.1 to 29.0% over the 4-week differentiation. HS 0S was the major HS disaccharide structure for all the differentiated states of CX cells, decreasing from 45.8 to 27.2% over the 4-week differentiation (Figure 3B). After the 4-week differentiation, the level of HS NS was also significantly reduced from 17.1 to 9.8%, and the level of HS NS2S decreased from 7.1 to 3.1%. CS 4S was present for all of the differentiated states, its level ranging from 3.9 to 7.5% (Figure 3C). After the 4-week differentiation, levels of CS 4S6S and 6S significantly increased from 0 and <1% to 12.1 and 5.0%, respectively.

We next characterized the GAGs from undifferentiated and 2-week and 4-week differentiated ReNcell VM human progenitor cells. The ReNcell VM cell line is derived from the ventral mesencephalon region of human fetal brain and is immortalized. It also possesses the capability of differentiating into neurons, astrocytes, and oligodendrocytes. HS the major GAG in VM cells, and its level increased from 80.5 to 85.5% after the 2-week differentiation and then decreased to 74.2% after the 4-week differentiation (Figure 4A). The total level of CS, however, increased from 5.1 to 10.1% after the 4-week differentiation, and the total level of HA fluctuated [14.5% (undifferentiated), 6.0% (2-week differentiation), and 15.7% (4-week differentiation)]. In VM cells, HS 0S is also the primary HS disaccharide, and its level fluctuated throughout the differentiation along with levels of HS NS and 6S (Figure 4B). The level of HS TriS, however, continuously decreased from 5.2 to 3.4% (2-week differentiation) and finally to 1.5% after the 4-week differentiation. The same trend was observed for HS NS6S; its level decreased from 9.4 to 2.6% (4-week differentiation). Small amounts (<1.5%) of HS NS2S and 2S were present in VM cells. CS 4S was the major CS disaccharide (~5%) and was found in all differentiation states and observed in CX cells (Figure 4C). CS 4S6S, 2S, and 0S were minor components (<1%), and the level of CS 6S significantly increased from 0.1 to 5.3% after a 4-week differentiation (Table 1).

Bovine eye GAGs were isolated from four different regions; conjunctiva, cornea, lens, and optic nerve were characterized by disaccharide analysis. Infections of conjunctiva and cornea are some of the most common and threatening routes of ocular tissue infection by pathogens.[31,32] CS was found to be the major GAG with levels of 75.3, 72.5, 38.8, and 72.9% in conjunctiva, cornea, lens, and optic nerve, respectively (Figure 5A). Other GAGs were also present in these tissues. In these

DOI: 10.1021/acs.biochem.8b01267
Biochemistry 2019, 58, 1155−1166

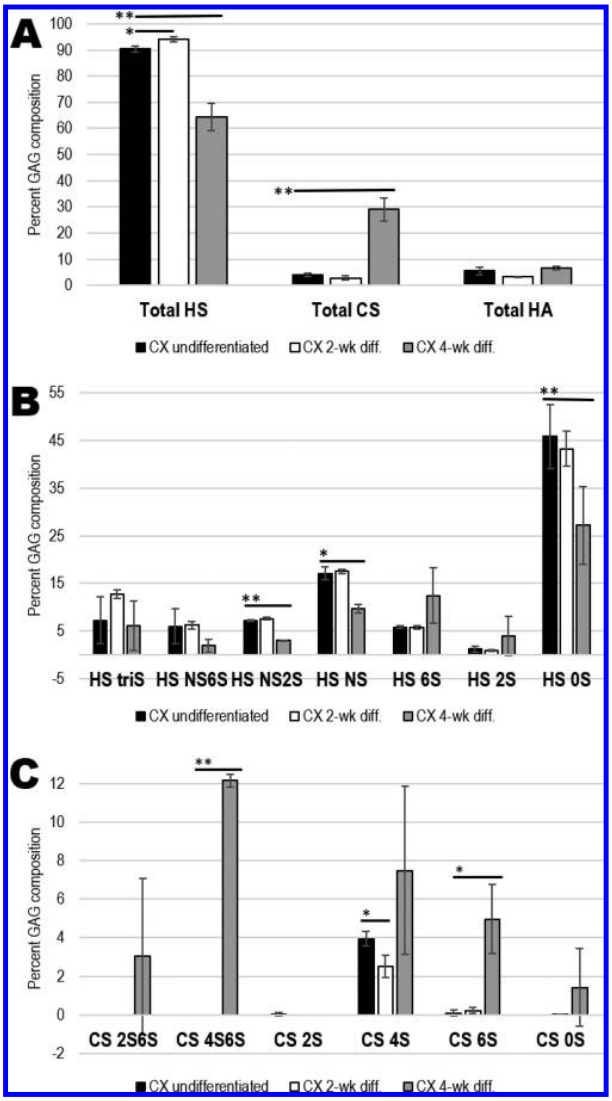

Figure 3. (A) Total GAG composition of CX (forebrain) cells. (B) HS disaccharide composition of CX cells. (C) CS disaccharide composition of CX cells. GAGs from three biological samples (grown in an individual tissue culture flask) were analyzed, and each sample was measured in triplicate. One asterisk and two asterisks denote the statistical comparison between undifferentiated and differentiated cells (2 and 4 weeks separately) (**$p < 0.01$; * $p < 0.05$).

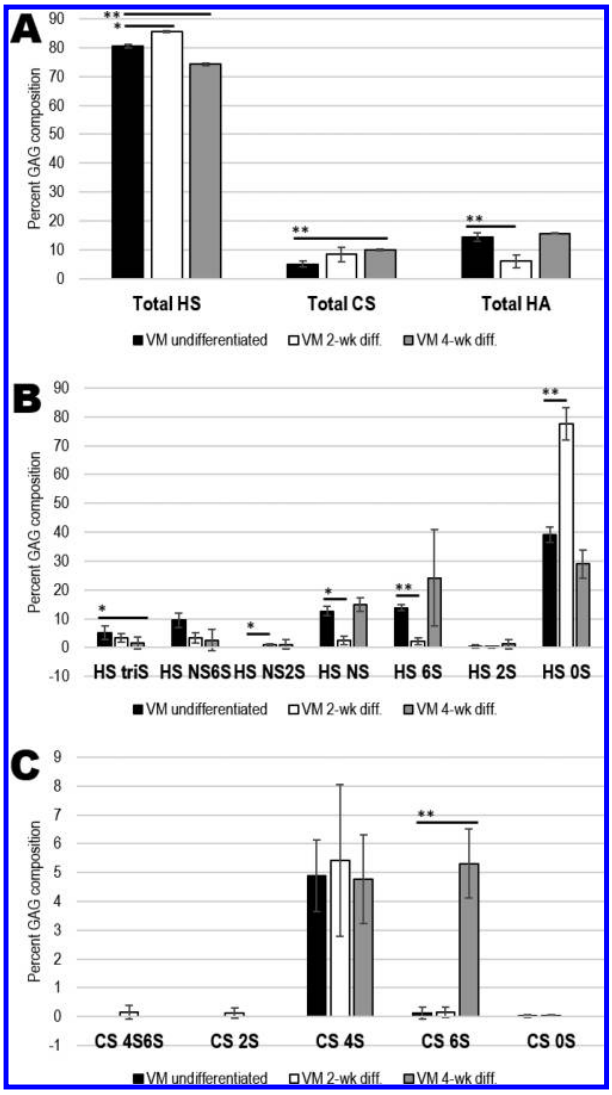

Figure 4. (A) Total GAG composition of VM (midbrain) cells. (B) HS disaccharide composition of VM cells. (C) CS disaccharide composition of VM cells. Each of the three biological samples was measured in triplicate. One asterisk and two asterisks denote statistical comparison between undifferentiated and differentiated cells (2 and 4 weeks separately) (**$p < 0.01$; *$p < 0.05$).

eye tissues, <10% of the GAGs were HS. Conjunctiva had 20.6% HA but very low levels of KS (0.3%). The GAG in optic nerve consisted of 17.9% HA and 0.5% total KS. In contrast, the GAGs in cornea were 1.3% HA and 24% KS. Finally, lens had both HA and KS at levels of 38.8 and 17.0%, respectively. The HS 2S6S disaccharide sequence was uniformly absent in all regions, and <1% HS TriS, NS6S, NS2S, NS, 6S, and 2S were present depending on the eye tissue (Figure 5B). HS 0S was the major HS disaccharide sequence, with levels of 2.3, 1.2, 5.4, and 6.0% for conjunctiva, cornea, lens, and optic nerve, respectively. CS 2S was uniformly absent in all regions, and the percent for CS triS, 2S4S, 2S6S, and 4S6S ranged from 0 to <3% (Figure 5C). CS 4S (CSA and/or CSB) was the major CS GAG in all four regions of the eye, with levels ranging from 24.8 to 60%; <1% CS 6S and <1% 0S were found in conjunctiva. In cornea, 3.6% CS 6S and 10% CS 0S were observed. In lens, 14% CS 0S was found while CS 6S was absent. The optic nerve showed <3% CS 6S and 0S. Conjunctiva and optic nerve had <1% KS (with both one and two sulfo groups), while the KS level for cornea and lens ranged from 4.4 to 16.6%. The percent composition of each disaccharide is shown in Table 2.

Antiviral assays followed treatment with four different heparin compounds, commercial unfractionated heparin (HP), low-molecular weight heparin (LMWH), heparin dodecasaccharides (dp12 HP), and s-NACH (non-anticoagulant heparin), differing in their chain length, sulfation, and disaccharide sequence.[26] HP dodecasaccharides were selected as they inhibited by >40% binding of ZIKV-EP to heparin in our previous studies.[10] Vero cells are widely accepted for use in the antiviral assay for pathogenic flaviviruses and were used to

DOI: 10.1021/acs.biochem.8b01267
Biochemistry 2019, 58, 1155−1166

Table 1. Disaccharide Analysis of VM and CX Cells throughout Various Differentiation Stages[a]

	undifferentiated VM	undifferentiated CX	2-week differentiated VM	2-week differentiated CX	4-week differentiated VM	4-week differentiated CX
HS TriS	5.16 ± 2.39	7.28 ± 4.94	3.37 ± 1.57	12.7 ± 0.94	1.47 ± 2.08	6.06 ± 5.21
HS NS6S	9.44 ± 2.51	6.03 ± 3.73	3.41 ± 1.72	6.26 ± 0.80	2.56 ± 3.62	1.94 ± 1.29
HS NS2S	0**	7.14 ± 0.15**	0.933 ± 0.28**	7.63 ± 0.24**	1.12 ± 1.6	3.07 ± 0.05
HS 2S6S	0	0	0	0	0	0
HS NS	12.7 ± 1.5	17.1 ± 1.4	2.38 ± 1.44*	17.6 ± 0.4*	14.8 ± 2.4	9.76 ± 0.90
HS 6S	13.9 ± 1.1**	5.84 ± 0.23**	2.28 ± 1.19	5.75 ± 0.34	24.17 ± 16.61	12.44 ± 5.83
HS 2S	0.329 ± 0.570	1.24 ± 0.61	0.093 ± 0.132**	0.939 ± 0.119**	1.17 ± 1.66	3.94 ± 4.08
HS 0S	39.04 ± 2.65	45.8 ± 6.7	77.6 ± 5.8	43.3 ± 3.6	29.0 ± 4.8	27.2 ± 8.2
HA	14.5 ± 1.5**	5.48 ± 1.35**	4.05 ± 2.20	3.15 ± 0.31	15.7 ± 0.14*	6.55 ± 0.640*
CS TriS	0	0	0	0	0	0
CS 2S4S	0	0	0	0	0	0
CS 2S6S	0	0	0	0	0	3.03 ± 4.045
CS 4S6S	0	0	0.161 ± 0.227	0	0**	12.14 ± 0.34**
CS 2S	0	0.053 ± 0.091	0.128 ± 0.181	0	0	0
CS 4S	4.90 ± 1.24	3.95 ± 0.39	5.41 ± 2.63	2.50 ± 0.57	4.77 ± 1.54	7.48 ± 4.35
CS 6S	0.126 ± 0.217	0.087 ± 0.151	0.168 ± 0.180	0.236 ± 0.150	5.31 ± 1.19	4.97 ± 1.79
CS 0S	0.028 ± 0.048	0	0.035 ± 0.018*	0.008 ± 0.013*	0	1.42 ± 2.01

[a]GAGs from three biological samples (grown in an individual tissue culture flask) were analyzed, and each sample was measured in triplicate. One asterisk and two asterisks denote statistical comparison between the disaccharide compositions of VM and CX cells (**$p < 0.01$; *$p < 0.05$).

test the antiviral activity of these heparin compounds against ZIKV.[21] The antiviral effect of HP was previously reported in DENV1−4, so DENV2 was included as a positive control in our assay for comparison.[7] In the first set of experiments, we tested 0.2−200 μg/mL HP, LMWH, dp12 HP, and s-NACH against ZIKV and DENV2 (Figure 6A,B). The compounds were added to Vero cells at the same time as the virus, and the supernatant was collected 48 h post-infection to determine virus titers by a plaque assay. For DENV2, all four compounds successfully reduced virus titer up to 93.5% at 200 μg/mL in a concentration-dependent manner (Figure 6A). The chain length of heparin (LMWH and dp12 HP) or the absence of an antithrombin binding site, in s-NACH, did not impact the ability of the heparin compound to inhibit DENV replication in Vero cells. Unexpectedly, in ZIKV, however, all heparin compounds tested promoted ZIKV replication in a concentration-dependent manner (Figure 6B). HP promoted ZIKV replication by 62, 47, 101, and 162.5% (1030000, 783000, 1680000, and 2710000 more PFU/mL than the control, respectively) at 0.2, 2, 20, and 200 μg/mL, respectively. LMWH also promoted ZIKV replication in Vero cells to a lesser extent, with levels ranging from 6.5 to 35% (108000 to 583000 more PFU/mL than the control, respectively). HP dodecasaccharide (dp12) had even less promotional activity for ZIKV replication. Between 0.2 and 20 μg/mL, dp12 HP inhibited ZIKV replication by 25−28% (417000−467000 fewer PFU/mL than the control); however, a higher concentration (200 μg/mL) led to a 35% increase (583000 more PFU/mL than the control) in ZIKV titer compared to that of the medium control. Finally, s-NACH promoted ZIKV replication by 58, 60, 86, and 126% (967000, 1000000, 1430000, and 2380000 more PFU/mL than the control, respectively) at 0.2, 2, 20, and 200 μg/mL, respectively, which are slightly lower than those of HP.

In the second set of experiments, we preincubated Vero cells with HP for 1 h prior to infection with ZIKV to emulate the patients given HP prior to ZIKV infection as a preventative therapeutic. We also examined a higher range of concentrations (100, 200, 500, and 1000 μg/mL) to determine if this would make a difference in its inhibitory/promotional activity with respect to ZIKV replication. Our results show that the ZIKV infection promotional activity was reduced when cells were pretreated with HP prior to ZIKV infection (Figure 6C). Compared to 162.5% promotion of ZIKV replication at 200 μg/mL upon addition to Vero cells with ZIKV simultaneously, HP had only 22%, or 2670000 more PFU/mL than the control (collected 48 h post-infection), and 52%, or 9000000 more PFU/mL than the control (72 h), promotional activity at 200 μg/mL in pretreated samples. Samples collected at 48 h had promotional activity up to 9.3%, which increased to 59% at 72 h. These results show that pretreatment of cells with HP prior to addition of ZIKV reduces the promotional activity of HP; however, it still does promote ZIKV replication, and a higher concentration of HP generally leads to higher promotional activity, not lower.

DISCUSSION

GAGs are utilized as attachment factors on the host cell surface during host cell invasion of various pathogenic flaviviruses, including DENV.[7,21] Previously, we characterized the structure of GAGs isolated from human placenta and tested their binding interactions with ZIKV-EP to investigate the association of human placental GAGs in the vertical transmission of ZIKV; however, GAGs from other tissues involved in ZIKV infection had not yet been analyzed.[10] In the first part of our study, we profiled the GAG disaccharide composition of the main vector of ZIKV, *Aedes* mosquitoes, in human fetal neural progenitor cells and bovine eye tissues known to be involved in the neural abnormalities caused by ZIKV infection.[5,12,16−18]

A. aegypti (AE) and *A. albopictus* (AL) are the main mosquito vectors of several pathogenic arboviruses, including DENV, CHIKV, and ZIKV; however, the systematic structural characterization of *Aedes* mosquito GAGs had not previously been performed.[5] Our findings show the order of GAG composition from largest to smallest as HS, HA, and CS in both *Aedes* mosquito species (Figure 2A). Both AE and AL showed comparable HS NS disaccharide compositions;

DOI: 10.1021/acs.biochem.8b01267
Biochemistry 2019, 58, 1155−1166

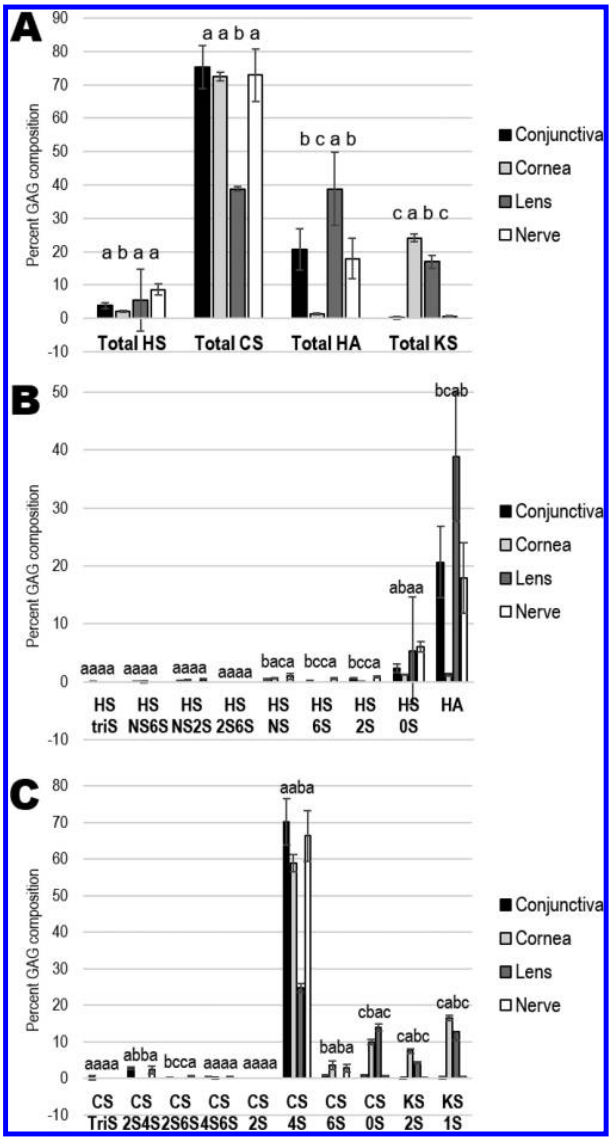

Figure 5. (A) Total GAG composition of bovine eyes. (B) HS and HA disaccharide composition of bovine eyes. (C) CS and KS disaccharide composition of bovine eyes. Glycosaminoglycans extracted from three sets of bovine eyes were analyzed (six samples per region), and each sample was measured in triplicate. The same subsets mean no statistically significant difference, while different subsets represent statistically significant differences.

however, notable differences between these two species were discovered. For example, a significantly higher level of HS 6S was observed in AE compared to the absence of HS 6S in AL (Figure 2B). AL, however, showed significantly higher levels of HS 0S. Similarly, nearly twice as much CS 4S was found in AL than in AE. Our previous findings for the *Anopheles stephensi* (AS) mosquito, a vector for congenital malaria caused by the *Plasmodium* parasite, showed that HS 0S and HS NS were also its major HS disaccharides.[30] However, the other major HS disaccharide in AS, HS NS6S, and minor HS disaccharides, HS TriS and NS2S, were not observed in either AE or AL. The major CS disaccharides in AS were CS 0S and CS 4S, but only CS 4S and small amounts of CS TriS were present in AE and AL.[30] In AS mosquitoes, the salivary gland basal lamina HS was found to be partly responsible for mediating midgut sporozoite invasion of this tissue.[33] In DENV, it was suggested that GAGs are not involved in the initial binding step of DENV replication in *Aedes* mosquitoes because the antiviral inhibitory activity of the polysaccharide ι-carrageenan is independent of the stage of DENV host cell invasion when it is added to mosquito cells (pre-infection, time of infection, or post-infection) and it showed reduced inhibitory activity in mosquito cells compared to that in Vero cells.[11] During the initial binding step of flavivirus infection, GAGs are known to interact with the virus mainly through electrostatic interaction with the surface EP. Previously, we learned that HS rich in TriS and HS 6S show a high affinity for ZIKV-EP, with HS rich in HS 0S showing a low affinity.[10] On the basis of GAG composition (significantly higher level of HS 6S and lower level of HS 0S), HS in *A. aegypti* mosquitoes might interact with ZIKV-EP with a slightly higher avidity in comparison with that of HS of *A. albopictus*. CSE (CS 4S6S) and CSB (CS 4S) were previously identified as high-affinity GAGs against ZIKV-EP; however, CS 4S (CSA and/or CSB) is present in small amounts in both species. Total high-affinity GAGs were present as minor components (<30%) in both species. As ZIKV-EP and DENV-EP exhibit structural similarities and binding against HP,[10] the relatively small amount of high-affinity GAGs against ZIKV-EP may partly explain the reduced level of involvement of GAGs during the initial binding step of DENV in host cell invasion in *Aedes* mosquitoes. The cellular substrate for generating virus can also modulate viral binding to host cell surface GAGs, replication, and virulence. CHIKV generated in *Aedes* mosquito cells (C6/36) loses its ability to bind to GAG and exhibits reduced infectivity; however, these are restored after a single passage in mammalian cells.[34] While no mutation has been reported in DENV generated in Vero or C6/36 cells, DENV generated in FRhL (fetal rhesus monkey lung) cells rapidly acquired a single Glu327Gly substitution in domain III of DENV-EP, which results in a significantly increased level of GAG binding.[35]

Next, we characterized human neural cell specific GAGs to investigate their potential role in developing brain and ZIKV pathogenesis. Brain development begins during the third gestational week that gives rise to neural progenitor cells and extends throughout adulthood.[36] Neurogenesis begins during the late embryonic period, while differentiation of astrocytes and oligodendrocytes is largely a postnatal process.[36] Human neural progenitor cells are preferential targets of ZIKV of all of the types of neural cells that ZIKV infects.[12−14] Human progenitor cell lines derived from cortical (CX) and ventral mesencephalon (VM) regions of human fetal brain during gestational weeks 14 and 10 were used to model neural cells of developing brain. We isolated GAGs from undifferentiated progenitor cells and 2-week and 4-week differentiated cells comprised of neurons, astrocytes, and oligodendrocytes for disaccharide composition analysis. With GAG profiles of CX and VM cells, we performed statistical analysis to evaluate the significant difference (1) between CX and VM cells (Table 1) and (2) between undifferentiated and differentiated states of each cell line (Figures 3 and 4). Comparison of high-affinity GAGs against ZIKV-EP of CX and VM cells reveals that HS 6S of undifferentiated VM exhibits a level significantly greater than that of CX (Table 1). While not statistically significant, undifferentiated VM has a lower level of HS TriS and a higher level of CS 4S compared to those of undifferentiated CX. In

DOI: 10.1021/acs.biochem.8b01267
Biochemistry 2019, 58, 1155−1166

Table 2. Disaccharide Analysis of Four Different Regions of Bovine Eyes (conjunctiva, cornea, lens, and optic nerve)[a]

GAG	conjunctiva	cornea	lens	optic nerve
HS TriS	0.034 ±0.084 a	0 a	0 a	0 a
HS NS6S	0.045 ± 0.037 a	0.001 ± 0.002 a	0 a	0 a
HS NS2S	0.194 ± 0.104 a	0.284 ± 0.056 a	0 a	0.285 ± 0.273 a
HS 2S6S	0 a	0 a	0 a	0 a
HS NS	0.394 ± 0.104 b	0.623 ± 0.086 a	0 c	0.931 ± 0.496 a
HS 6S	0.227 ± 0.049 b	0 c	0 c	0.535 ± 0.102 a
HS 2S	0.583 ± 0.049 b	0.014 ± 0.033 c	0 c	0.824 ± 0.123 a
HS 0S	2.315 ± 0.687 a	1.205 ± 0.139 b	5.358 ± 9.27 a	6.025 ± 0.863 a
HA	20.65 ± 6.22 b	1.26 ± 0.232 c	38.823 ± 11.06 a	17.931 ± 6.081 b
CS TriS	0.218 ± 0.534 a	0 a	0 a	0 a
CS 2S4S	2.755 ± 0.415 a	0 b	0 b	2.327 ± 1.058 a
CS 2S6S	0.187 ± 0.045 b	0 c	0 c	0.694 ± 0.107 a
CS 4S6S	0.319 ± 0.171 a	0.045 ± 0.109 a	0 a	0.256 ± 0.192 a
CS 2S	0 a	0 a	0 a	0 a
CS 4S	70.134 ± 6.39 a	58.862 ± 2.284 a	24.826 ± 1.174 b	66.262 ± 6.849 a
CS 6S	0.983 ± 0.097 b	3.628 ± 1.200 a	0 b	2.765 ± 1.054 a
CS 0S	0.702 ± 0.343 c	9.977 ± 0.724 b	13.988 ± 0.931 a	0.642 ± 0.125 c
KS 2S	0.07 ± 0.101 c	7.547 ± 0.601 a	4.356 ± 0.217 b	0.109 ± 0.073 c
KS 1S	0.19 ± 0.303 c	16.554 ± 0.724 a	12.649 ± 2.127 b	0.414 ± 0.210 c

[a]Glycosaminoglycans extracted from three sets of bovine eyes were analyzed (six samples per region), and each sample was measured in triplicate. The same subsets mean no statistically significant difference, while different subsets represent statistically significant differences.

the 4-week differentiation period, higher levels of all high-affinity GAGs against ZIKV-EP, except that of HS 6S, were observed in CX cells than in VM cells. The total amount of high-affinity GAGs was larger in undifferentiated VM cells (23.89%) than in undifferentiated CX cells (17.07%); however, this order changed during the 4-week differentiation periods. Given that high-affinity GAGs against ZIKV-EP are not present as major GAGs in neural progenitor and differentiated cell samples, GAGs may not play the role of attachment factors for ZIKV to target during the adsorption step of host cell invasion. Next, we compared GAG levels of undifferentiated from differentiated for each cell line. In CX cells, the level of 6S was found to be greater in 4-week differentiated cells. The level of CS 4S6S of 4-week differentiated cells was statistically greater than that of undifferentiated cells. The level of CS 4S was also found to be significantly lower in 2-week differentiated cells. In VM cells, significantly lower levels of HS TriS and 6S were found in differentiated cells. Immature cortical neurons differentiated from human neural progenitor cells have been reported to exhibit a lower level of ZIKV infection, while human neural progenitor cells show excellent permissiveness.[12] These changes in the GAG profile between undifferentiated and differentiated cells may partly explain this difference in permissiveness in ZIKV infection.

We then analyzed ocular specific GAGs, as ocular abnormalities were also found in infants affected by vertical ZIKV transmission.[16−18] GAGs in the cornea, retina, and vitreous humor of the eye were previously reported, and the main GAGs in each region were KS and CS, CS (CS 0S and 6S), and HA, respectively.[37−39] However, a systematic characterization of GAG disaccharides of conjunctiva, lens, and optic nerve had not previously been reported. CS was the major GAG in all four isolated regions of the eye (conjunctiva, cornea, lens, and optic nerve); however, the other main GAG partner in each region varied (Figure 5A). For the conjunctiva and optic nerve, CS and HA were the main GAGs. In the cornea, CS and KS were the main GAGs. Interestingly, lens exhibited similar levels of total CS, HA, and KS. In all regions of the eye, HS was a minor component, with HS 0S being the main HS disaccharide (Figure 5B). In contrast, CS 4S was the main CS disaccharide in all four regions (Figure 5C). In our previous studies, CS 4S was also found to be the major GAG/CS disaccharide in the human placenta, which interacted with ZIKV-EP at subnanomolar affinity.[10] The CS 4S found in bovine eye can be CSA and/or CSB in its disaccharide structure, which could potentially also interact with ZIKV-EP and assist in ZIKV pathogenesis.

In addition to cell/tissue specific GAG characterization, we performed an *in vitro* antiviral assay on heparin compounds with various structures (HP, LMWH, dp12 HP, and s-NACH) against ZIKV and DENV2 infection in Vero cells. HP previously has been reported to show antiviral activity against both ZIKV and DENV1−4 in Vero cells.[7,21,23] HP dp12 competitively inhibits the binding of ZIKV-EP to HP by >40%, and shorter chain length oligosaccharides are advantageous as a therapeutic option due to their reduced anticoagulant activity.[10] Thus, we tested a set of HPs varying in their chain length, number of sulfate groups, and disaccharide sequence to better understand the minimal chain length and structure required for effective antiviral activity against ZIKV and DENV2 infection *in vitro*. In the first set of our study, we added the compounds and the virus to Vero cells at the same time, the supernatant was collected 48 h post-infection, and the virus titer was measured. Independent of chain length or disaccharide sequence, all four compounds showed excellent antiviral activity against DENV2 up to 93.5% at 200 μg/mL in a concentration-dependent manner, showing that the chain length of HP dp12 is sufficient to result in an antiviral activity equivalent to that of commercial unfractionated HP with a longer average chain length (Figure 6A). Surprisingly, the same compounds showed the opposite effect when used in ZIKV infection where viral replication was promoted, rather than inhibited, in a concentration-dependent manner (Figure 6B). This promotional activity was also dependent upon the structure of the compounds. HP, LMWH, and HP dp12 share the same main disaccharide sequence of →4)-*N*-sulfo 6-

DOI: 10.1021/acs.biochem.8b01267
Biochemistry 2019, 58, 1155−1166

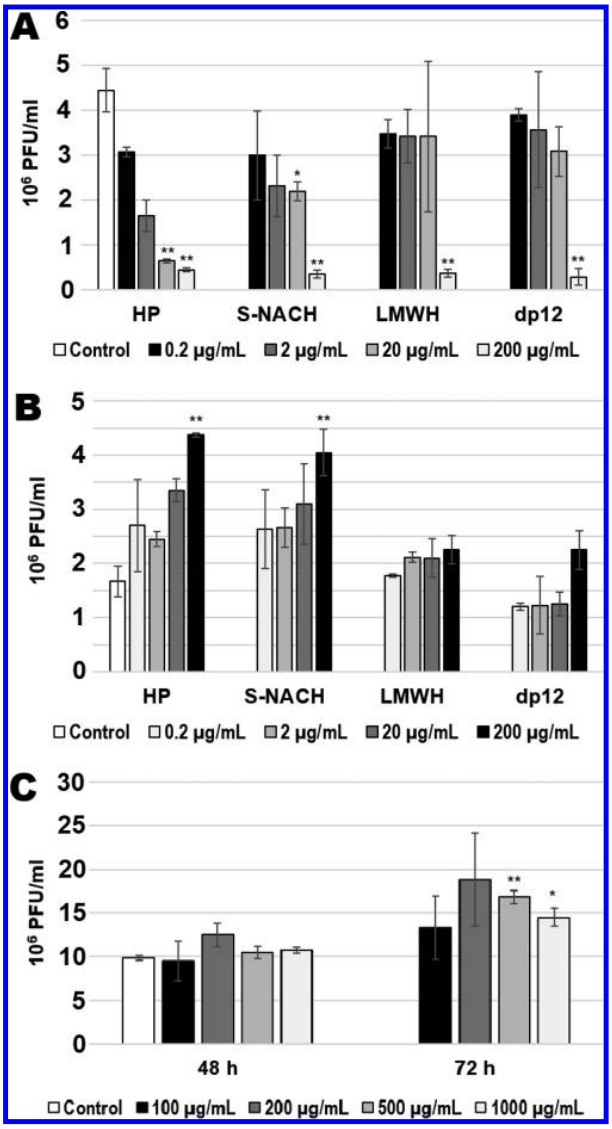

Figure 6. Viral reduction antiviral assay of heparin (HP), low-molecular weight heparin (LMWH), non-anticoagulant heparin (s-NACH), and heparin dodecasaccharide (dp12) in (A) DENV2 and (B) ZIKV. (C) Viral reduction antiviral assay in ZIKV in which heparin was preincubated with Vero cells 1 h prior to ZIKV infection. The control condition included virus and medium (no antiviral compound added). A single experiment was performed in triplicate. One asterisk and two asterisks denote statistical comparison between the control and each sample (**$p < 0.01$; *$p < 0.05$).

O-sulfo-α-D-glucosamine-(1→4)-2-*O*-sulfo α-L-iduronic acid-(1→ but vary in chain length, and they also show differences in the total number of sulfate groups per molecule. Our results suggest that longer chain length HP has greater proviral activity for ZIKV replication in Vero cells. A non-anticoagulant heparin, s-NACH, lacking an antithrombin III binding site, may be useful in patients infected with DENV showing symptoms of hemorrhagic fever.[26] s-NACH also promoted ZIKV replication in Vero cells in a concentration-dependent manner but to a slightly lesser extent, suggesting that the lack of an antithrombin binding site does not affect the promotional outcome in ZIKV replication. These results may not be comparable to those of a previous study in which HP was incubated with ZIKV for 1 h prior to being added to Vero cells; however, this is the first report of HP promoting flaviviral replication.

In a second set of experiments, we incubated Vero cells with HP for 1 h prior to ZIKV infection and the supernatant was collected 48 and 72 h post-infection for the plaque assay (Figure 6C). The HP promotional activity was slightly lower upon preincubation of the cells prior to infection in comparison with that for simultaneous addition with virus at the time of infection. However, HP still promoted ZIKV replication, which progressed further 72 h post-infection (Figure 6C). This incubation method mirrors the condition used in the study in which HP reduced ZIKV-induced cytopathic effects when preincubated for 1 h prior to infection of human neural progenitor cells.[22] In their study, samples were collected at 72 and 168 h. A 1 h treatment of neural progenitor cells with 100 μg/mL HP prior to infection results in a 2−3-fold decrease in ZIKV titer.[22] In our study, 100 μg/mL HP promoted ZIKV replication in Vero cells by 29% at 72 h post-infection (Figure 6C). At 500 and 1000 μg/mL, HP results in statistically different ZIKV titers in comparison with that of the control. The anti- or proviral function of HP in ZIKV replication suggests that (1) the role of GAGs as attachment factors in ZIKV host cell invasion may depend on the structure of cell/tissue specific GAGs and (2) GAGs may exhibit alternative roles in ZIKV pathogenesis through other mechanisms, such as cellular signaling. While HP is thought to work as a competitive inhibitor against binding of EP to host cell surface GAGs during DENV and other flaviviral infection, it may work differently in the case of ZIKV. Our GAG disaccharide compositional analysis revealed that ZIKV-EP high-affinity GAGs are not present in large amounts in the GAGs of human fetal neural progenitor cells (Figures 3B and 4B), yet HP was able to moderately inhibit ZIKV replication and ZIKV-induced cell death in human neural progenitor cells as suggested by the work of Ghezzi et al., who suggested that there may be an alternate mode of action.[22] Additionally, HP works as a proviral agent in Vero cells, further confirming that interference with EP binding may not be the controlling mechanism.

In conclusion, we characterized the GAG disaccharide composition of *A. aegypti* and *A. albopictus* mosquitoes, human fetal neural progenitor cells and differentiated astrocytes, neurons, and oligodendrocytes, and bovine eye tissues to investigate their relevance in ZIKV pathogenesis. We also tested HP compounds of varying structure for *in vitro* antiviral activity against ZIKV and DENV2 infection in Vero cells and found that HP exhibits structure specific proviral activity for ZIKV replication in a concentration-dependent manner in contrast to the antiviral activity shown against DENV2. HP dp12 shows an antiviral activity comparable to that of commercial unfractionated HP against DENV2 infection. Our study further expands our understanding of the involvement of GAGs in ZIKV pathogenesis and may contribute to the rational design of carbohydrate-based therapeutics against flaviviral transmission.

■ ASSOCIATED CONTENT

Supporting Information

The Supporting Information is available free of charge on the ACS Publications website at DOI: 10.1021/acs.biochem.8b01267.

DOI: 10.1021/acs.biochem.8b01267
Biochemistry 2019, 58, 1155−1166

Western blots and densitometry analysis of ReNcell VM and CX markers (PDF)

AUTHOR INFORMATION

Corresponding Authors

*Department of Chemistry and Chemical Biology, Center for Biotechnology and Interdisciplinary Studies, Rensselaer Polytechnic Institute, Troy, NY 12180. E-mail: zhangf2@rpi.edu. Telephone: (518) 276-3404. Fax: (518) 276-3405.
*E-mail: linhar@rpi.edu.

ORCID

Jonathan S. Dordick: 0000-0001-7802-3702
Fuming Zhang: 0000-0003-2803-3704
Robert J. Linhardt: 0000-0003-2219-5833

Funding

This research was funded by National Institutes of Health Grants DK111958, CA231074, HL125371, and NS088496.

Notes

The authors declare no competing financial interest.

ABBREVIATIONS

AE, *A. aegypti*; AL, *A. albopictus*; AMAC, 2-aminoacridone; AS, *An. stephensi*; CHAPS, 3-[(3-cholamidopropyl)-dimethylammonio]-1-propanesulfonate; CHIKV, Chikungunya virus; CN, conjunctiva; CR, cornea; CS, chondroitin sulfate; DENV, Dengue virus; dp, degree of polymerization; dpi, day(s) post-infection; EC, effective concentration; EDC, 1-ethyl-3-[3-(dimethylamino)propyl]carbodiimide; EGF, epidermal growth factor; EP, envelope protein; FGF, fibroblast growth factor; FGFR, fibroblast growth factor receptor; FBS, fetal bovine serum; GAG, glycosaminoglycan; HA, hyaluronic acid; hNPC, human neural progenitor cell; HS, heparan sulfate; HP, heparin; IC, inhibitory concentration; JEV, Japanese encephalitis virus; KS, keratan sulfate; L, lens; LC−MS, liquid chromatography−mass spectrometry; LIF, leukemia inhibitory factor; LMWH, low-molecular weight heparin; MOI, multiplicity of infection; MWCO, molecular weight cutoff; N, optic nerve; NHS, *N*-hydroxysuccinimide; PBS, phosphate-buffered saline; PG, proteoglycan; RU, resonance unit; SDS, sodium dodecyl sulfate; s-NACH, non-anticoagulant heparin; SPR, surface plasmon resonance; VEGF, vascular endothelial growth factor; WNV, West Nile virus; YFV, yellow fever virus; ZIKV, Zika virus.

REFERENCES

(1) Sirohi, D., Chen, Z., Sun, L., Klose, T., Pierson, T. C., Rossmann, M. G., and Kuhn, R. J. (2016) The 3.8 Å resolution cryo-EM structure of Zika virus. *Science 352*, 467−70.

(2) Sirohi, D., and Kuhn, R. J. (2017) Zika virus structure, maturation, and receptors. *J. Infect. Dis. 216*, S935−S944.

(3) Magnus, M. M., Espósito, D. L. A., Costa, V. A., Silva de Melo, P. S., Costa-Lima, C., Fonseca, B. A. L. da, and Addas-Carvalho, M. (2018) Risk of Zika virus transmission by blood donations in Brazil. *Hematology, Transfusion and Cell Therapy 40*, 250−254.

(4) D'Ortenzio, E., Matheron, S., de Lamballerie, X., Hubert, B., Piorkowski, G., Maquart, M., Descamps, D., Damond, F., Yazdanpanah, and Leparc-Goffart, I. (2016) Evidence of sexual transmission of Zika virus. *N. Engl. J. Med. 374*, 2195−2198.

(5) Ciota, A. T., Bialosuknia, S. M., Zink, S. D., Brecher, M., Ehrbar, D. J., Morrissette, M. N., and Kramer, L. D. (2017) Effects of Zika virus strain and Aedes mosquito species on vector competence. *Emerging Infect. Dis. 23*, 1110−1117.

(6) Rice, M. E., Galang, R. R., Roth, N. M., Ellington, S. R., Moore, C. A., Valencia-Prado, M., Ellis, E. M., Tufa, A. J., Taulung, L. A., Alfred, J. M., Perez-Padilla, J., Delgado-Lopez, C. A., Zaki, S. R., Reagan-Steiner, S., Bhatnagar, J., Nahabedian, J. F., Reynolds, M., Yeargin-Allsopp, M., Viens, L. J., Olson, S. M., Jones, A. M., Baez-Santiago, M. A., Oppong-Twene, P., Simon, E. L., Moore, J. T., Polen, K. D., Hillman, B., Ropeti, R., Nieves-Ferrer, L., Marcano-Huertas, M., Masao, C., Anzures, E. J., Hansen, R. L., Perez-Gonzalez, S. I., Espinet-Crespo, C. P., Luciano-Roman, M., Shapiro-Mendoza, C. K., Gilboa, S. M., and Honein, M. A. (2018) Vital signs: Zika-associated birth defects and neurodevelopmental abnormalities possibly associated with congenital Zika virus infection — U.S. territories and freely associated States, 2018. *Morbidity and Mortality Weekly Report 67*, 858−867.

(7) Chen, Y., Maguire, T., Hileman, R. E., Fromm, J. R., Esko, J. D., Linhardt, R. J., and Marks, R. M. (1997) Dengue virus infectivity depends on envelope protein binding to target cell heparan sulfate. *Nat. Med. 3*, 866−871.

(8) Kamhi, E., Joo, E. J., Dordick, J. S., and Linhardt, R. J. (2013) Glycosaminoglycans in infectious disease. *Biol. Rev. 88*, 928−943.

(9) Linhardt, R. J., and Toida, T. (2004) Role of glycosaminoglycans in cellular communication. *Acc. Chem. Res. 37*, 431−438.

(10) Kim, S. Y., Zhao, J., Liu, X., Fraser, K., Lin, L., Zhang, X., Zhang, F., Dordick, J. S., and Linhardt, R. J. (2017) Interaction of Zika virus envelope protein with glycosaminoglycans. *Biochemistry 56*, 1151−1162.

(11) Talarico, L. B., Noseda, M. D., Ducatti, D. R. B., Duarte, M. E. R., and Damonte, E. B. (2011) Differential inhibition of dengue virus infection in mammalian and mosquito cells by iota-carrageenan. *J. Gen. Virol. 92*, 1332−1342.

(12) Tang, H., Hammack, C., Ogden, S. C., Wen, Z., Qian, X., Li, Y., Yao, B., Shin, J., Zhang, F., Lee, E. M., Christian, K. M., Didier, R. A., Jin, P., Song, H., and Ming, G. (2016) Zika virus infects human cortical neural progenitors and attenuates their growth. *Cell Stem Cell 18*, 587−590.

(13) Lin, M.-Y., Wang, Y.-L., Wu, W.-L., Wolseley, V., Tsai, M.-T., Radic, V., Thornton, M. E., Grubbs, B. H., Chow, R. H., and Huang, I.-C. (2017) Zika virus infects intermediate progenitor cells and post-mitotic committed neurons in human fetal brain tissues. *Sci. Rep. 7*, 14883.

(14) Muffat, J., Li, Y., Omer, A., Durbin, A., Bosch, I., Bakiasi, G., Richards, E., Meyer, A., Gehrke, L., and Jaenisch, R. (2018) Human induced pluripotent stem cell-derived glial cells and neural progenitors display divergent responses to Zika and dengue infections. *Proc. Natl. Acad. Sci. U. S. A. 115*, 7117−7122.

(15) Rowlands, D., Sugahara, K., and Kwok, J. C. F. (2015) Glycosaminoglycans and glycomimetics in the central nervous system. *Molecules 20*, 3527−3548.

(16) de Paula Freitas, B., de Oliveira Dias, J. R. J., Prazeres, J., Sacramento, G. A. G., Ko, A. I., Maia, M. M., and Belfort, R. J. (2016) Ocular Findings in Infants With Microcephaly Associated With Presumed Zika Virus Congenital. *JAMA Ophthalmol. 134*, 529−35.

(17) Ventura, C. V., Maia, M., Bravo-Filho, V., Góis, A. L., and Belfort, R. (2016) Zika virus in Brazil and macular atrophy in a child with microcephaly. *Lancet 387*, 228.

(18) Jampol, L. M., and Goldstein, D. A. (2016) Zika virus infection and the eye. *JAMA Ophthalmol. 134*, 535−536.

(19) Park, P. J., and Shukla, D. (2013) Role of heparan sulfate in ocular diseases. *Exp. Eye Res. 110*, 1−9.

(20) Yamada, S., Sugahara, K., and Özbek, S. (2011) Evolution of glycosaminoglycans: Comparative biochemical study. *Commun. Integr. Biol. 4*, 150−158.

(21) Kim, S. Y., Li, B., and Linhardt, R. J. (2017) Pathogenesis and inhibition of flaviviruses from a carbohydrate perspective. *Pharmaceuticals 10*, 44.

(22) Ghezzi, S., Cooper, L., Rubio, A., Pagani, I., Capobianchi, M. R., Ippolito, G., Pelletier, J., Meneghetti, M. C. Z., Lima, M. A., Skidmore, M. A., Broccoli, V., Yates, E. A., and Vicenzi, E. (2017)

DOI: 10.1021/acs.biochem.8b01267
Biochemistry 2019, 58, 1155−1166

Heparin prevents Zika virus induced-cytopathic effects in human neural progenitor cells. *Antiviral Res. 140*, 13−17.
(23) Tan, C. W., Sam, I. C., Chong, W. L., Lee, V. S., and Chan, Y. F. (2017) Polysulfonate suramin inhibits Zika virus infection. *Antiviral Res. 143*, 186−194.
(24) Lane, D. a, Denton, J., Flynn, a M., Thunberg, L., and Lindahl, U. (1984) Anticoagulant activities of heparin oligosaccharides and their neutralization by platelet factor 4. *Biochem. J. 218*, 725−32.
(25) Linhardt, R. J., Rice, K. G., Kim, Y. S., Engelken, J. D., and Weiler, J. M. (1988) Homogeneous, structurally defined heparin-oligosaccharides with low anticoagulant activity inhibit the generation of the amplification pathway C3 convertase in vitro. *J. Biol. Chem. 263*, 13090−13096.
(26) Islam, T., Butler, M., Sikkander, S. A., Toida, T., and Linhardt, R. J. (2002) Further evidence that periodate cleavage of heparin occurs primarily through the antithrombin binding site. *Carbohydr. Res. 337*, 2239−2243.
(27) Linhardt, R. J., Turnbull, J. E., Wang, H. M., Loganathan, D., and Gallagher, J. T. (1990) Examination of the substrate specificity of heparin and heparan sulfate lyases. *Biochemistry 29*, 2611−2617.
(28) Wang, H., He, W., Jiang, P., Yu, Y., Lin, L., Sun, X., Koffas, M., Zhang, F., and Linhardt, R. J. (2017) Construction and functional characterization of truncated versions of recombinant keratanase II from Bacillus circulans. *Glycoconjugate J. 34*, 643−649.
(29) Kauffman, E., Payne, A., Franke, M. A., Schmid, M. A., Harris, E., and Kramer, L. D. (2017) Rearing of Culex spp. and Aedes spp. mosquitoes. *Bio-Protoc. 7*, e2542.
(30) Sinnis, P., Coppi, A., Toida, T., Toyoda, H., Kinoshita-Toyoda, A., Xie, J., Kemp, M. M., and Linhardt, R. J. (2007) Mosquito heparan sulfate and its potential role in malaria infection and transmission. *J. Biol. Chem. 282*, 25376−25384.
(31) Belser, J. A., Rota, P. A., and Tumpey, T. M. (2013) Ocular tropism of respiratory viruses. *Microbiol. Mol. Biol. Rev. 77*, 144−156.
(32) Teweldemedhin, M., Gebreyesus, H., Atsbaha, A. H., Asgedom, S. W., and Saravanan, M. (2017) Bacterial profile of ocular infections: A systematic review. *BMC Ophthalmol. 17*, 1−9.
(33) Armistead, J. S., Wilson, I. B. H., van Kuppevelt, T. H., and Dinglasan, R. R. (2011) A role for heparan sulfate proteoglycans in *Plasmodium falciparum* sporozoite invasion of anopheline mosquito salivary glands. *Biochem. J. 438*, 475−483.
(34) Acharya, D., Paul, A. M., Anderson, J. F., Huang, F., and Bai, F. (2015) Loss of glycosaminoglycan receptor binding after mosquito cell passage reduces chikungunya virus infectivity. *PLoS Neglected Trop. Dis. 9*, e0004139.
(35) Anez, G., Men, R., Eckels, K. H., and Lai, C.-J. (2009) Passage of Dengue Virus Type 4 Vaccine Candidates in Fetal Rhesus Lung Cells Selects Heparin-Sensitive Variants That Result in Loss of Infectivity and Immunogenicity in Rhesus Macaques. *J. Virol. 83*, 10384−10394.
(36) Stiles, J., and Jernigan, T. L. (2010) The basics of brain development. *Neuropsychol. Rev. 20*, 327−348.
(37) Peng, Y., Yu, Y., Lin, L., Liu, X., Zhang, X., Wang, P., Hoffman, P., Kim, S. Y., Zhang, F., and Linhardt, R. J. (2018) Glycosaminoglycans from bovine eye vitreous humour and interaction with collagen type II. *Glycoconjugate J. 35*, 119−128.
(38) Inatani, M., and Tanihara, H. (2002) Proteoglycans in retina. *Prog. Retinal Eye Res. 21*, 429−447.
(39) Sridhar, M. S. (2018) Anatomy of cornea and ocular surface. *Indian J. Ophthalmol. 66*, 190−194.

DOI: 10.1021/acs.biochem.8b01267
Biochemistry 2019, 58, 1155−1166